

Accurate Matlab/Simulink model of a Power Generation System Based on Fuel Cells

A. S. Carvalho, Member IEEE, M.T. Outeiro

Department of Electrical Engineering and Computers, Engineering Faculty of Oporto University, Porto, Portugal

E-mail: asc@fe.up.pt

Institute of Systems and Robotics, University of Porto, Portugal

E-mail: teresa.outeiro@fe.up.pt

Abstract- Modeling and simulation techniques are indispensable in every aspect of power system design. Power systems need to be simulated in a longer period of time and more frequently especially when they are being analyzed using complex computer algorithms.

The MatLab/Simulink software is used in the simulation of a power generation system based on fuel cells. To provide a higher level of accuracy, a stiff algorithm is used. The accuracy of the simulation is verified by comparing the simulation results to those obtained experimentally in a prototype.

Firstly the paper presents the electrical equivalent circuit of the PEM fuel cell, and its modelization in MatLab/Simulink.

Secondly and once selected the topology and decided the control structure of the converter, its implementation in MatLab/Simulink software is presented. The model of the power generation system is performed in two parts, namely: the power circuit and the control circuit

A special attention is given to the control strategy, providing detailed explanation to each control subsystem, particularly, the voltage control, the frequency control and PEM control.

The simulation and experimental results that are focused on the stability of the system, and the resonant converter operation, are used to validate the accuracy of the model developed.

NOMENCLATURE

A	cell active area (cm ²)
C	equivalent electrical capacitance (F)
E_{Nernst}	thermodynamic potential
J_{max}	maximum current density (A/cm ²)
n	number of cells in stack
P_{O_2}	oxygen partial pressure (atm)
P_{H_2}	hydrogen partial pressure (atm)
R_C	contact resistance (Ω)
R_M	equivalent membrane resistance (Ω)
T	cell operating temperature (K)
V_{act}	activation voltage drop (V)
V_{ohmic}	ohmic voltage drop (V)
V_{con}	concentration voltage (V)
ξ_i, ψ	parametric coefficients
λ	membrane thickness (μ m)
f_r	resonant frequency (Hz)
Z_r	resonant impedance (Ω)
L_r	resonant tank inductor (H)
C_r	resonant tank capacitor (F)
Q	quality factor

I. INTRODUCTION

The analysis, design and practical implementation of power converters without computer simulation are extremely laborious, time-consuming and expensive. Thus computer simulation plays an important role in the design and analysis of these converters and their controllers [1,2].

In this paper a power generation systems based on fuel cells is carried out and its performance is evaluated in simulation and experimentally. The MatLab/Simulink software [3] is a package designed for modelling, simulating and analyzing dynamic systems, it supports linear and nonlinear systems modeled in continuous time, sampled time or a combination of both, therefore it is well suited to modelling and simulating converters and controllers in the analogue and digital domains.

In the case of a power generation system based on fuel cell, the fuel cell process involved inside the fuel cell is complex and nonlinear, with multi-variables involved, which usually lead to nonlinear parameter estimation problems, which often contain more than one minimum. The simulated annealing, SA is a method characterized by its ability to trap in local minimum, as well as its flexibility and robustness. The SA has been implemented in the MatLab/Simulink software to solve the problem of identification of the PEM fuel cell parameters, whose results are presented in [4,5].

The power electronic converter plays an important role on the interface of the fuel cell system as power generating system. The fuel cell output voltage varies normally in the range of 20–50V. There are several possible converter topologies that can be used: DC-DC together with DC-AC (Figure 1), DC-AC interfacing directly the fuel cell to the grid (Figure 2), or DC-DC together with AC-AC isolated by a transformer (Figure 3). A specific application must be considered in order to select the best topology [6-8]. Usually the DC-DC converter is put between the fuel cell and the inverter which performs two functions: 1) acts as the DC isolation for the inverter; and 2) produces sufficient voltage for the inverter input so that the required magnitude of the AC voltage can be produced [9]. The selection of the topology is based on some criteria, which is also analyzed in the paper.

The paper is organized as follows; in Section II the PEM fuel cell is characterized and its MatLab/Simulink model is presented. The Section III is dedicated to the converter namely, the selection of the topology, operating principle and control. The details of the converter model and control

implementation in the MatLab/Simulink software are presented in Section IV and the simulation and experimental results are shown in Sections V and VI respectively. The Section VII presents the conclusions.

A. PEM FUEL CELL

II. Modelling of the PEM fuel cell

In order to control fuel cells, it is useful first to present a dynamic model, in order to better understand the system. The authors and others have developed a model previously, adopting the electrochemical equivalent circuit of Figure 4. This circuit can be used for the static and dynamic analysis of the behavior of a PEM fuel cell. Its numerical representation is described by a set of equations, which are summarized in Table 1. These equations and correspondent parameter values are essential for the analysis and control of the PEM performance.

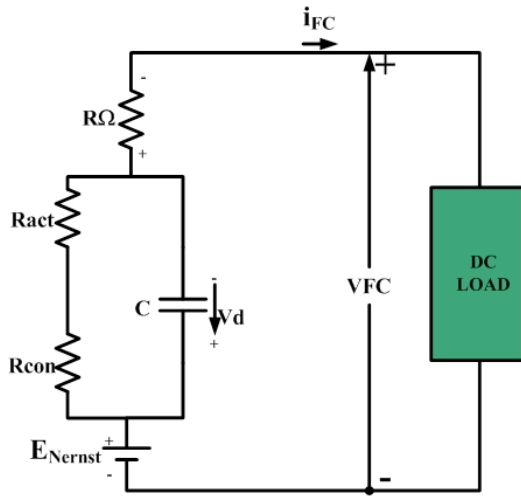


Fig. 1 – A simplified model of the PEM with only one cell.

The performance can be measured by the relationship between hydrogen consumption and its output power (P_{FC}). High efficiency means low hydrogen consumption. the hydrogen consumption is the difference between the flow input and output flow of hydrogen. However, the energy conversions will lead to a certain amount of quality degradation, that is, the input power will not all transferred to the output. The maximum of output power means minimum of losses and there are two kinds of losses: the hydrogen losses and the electrical losses.

Small amounts of hydrogen that feed in the stack to be converted to electric power will however be purged out of the system. The net power delivered from the system will be slightly lower because of this loss. The overall efficiency of the system must take all these losses into account. The hydrogen consumed by Mark1020 PEM, according to the current, is shown in the results section of the paper. The electrical power (P_{FC}) supplied by the fuel cell is determined by equation 9 while equation 10 corresponds to the efficiency of the fuel cell system.

Table 1: Summary of the equations used in the model.

Static Equations	
Output voltage of one single cell	$V_{FC} = E_{Nernst} - V_{act} - V_{Ohmic} - V_{con}$ (1)
Thermodynamic potential	$E_{Nernst} = 1.229 - 0.85 \times 10^{-3} \times (T - 298.15) + 4.31 \times 10^{-5} \times T \times \left[\ln(P_{H_2}) + \frac{1}{2} \ln(P_{O_2}) \right]$ (2)
Activation over-potential	$V_{act} = -\left[\xi_1 + \xi_2 \times T + \xi_3 \times T \times \ln(CO_2) + \xi_4 \times T \times \ln(i_{FC}) \right]$ (3)
Ohmic over-potential	$V_{ohmic} = i_{FC} (R_M + R_C)$ (4)
Concentration over potential	$V_{con} = -B \times \ln\left(1 - \frac{J}{J_{max}}\right)$ (5)
Output voltage of the stack	$V_s = n \times V_{FC}$ (6)
Dynamic Equations	
Dynamical voltage across the capacitor	$\frac{dV_d}{dt} = \left(\frac{1}{C} \times i_{FC}\right) - \left(\frac{1}{\tau} \times V_d\right)$ (7)
Electrical Time-constant	$\tau = C \times Ra = C \times (R_{act} + R_{con})$ (8)
Performance	
Electrical power	$P_{FC} = i_{FC} \times V_{FC}$ (9)
Efficiency	$\eta_{el} = \mu_f \times \left(\frac{V_{FC}}{1.48}\right) \times 100\%$ (10)

III. Model of the PEM fuel cell in Matlab/simulink

The model of the PEM is implemented in MatLab/Simulink as a voltage-source controlled in current. It is composed by two subsystems, as shown in Figure 2. The static model and the dynamic model are implemented by the equations of the electrochemical equivalent circuit defined in the previous section. As can be observed the output signals of the static model are used as the input signals of the dynamic model, accordingly to the analytical formulation. The optimal parameters found by the SA algorithm are used in this model and the temperature is considered by an input variable, defined by a vector associated with PEM to analyze.

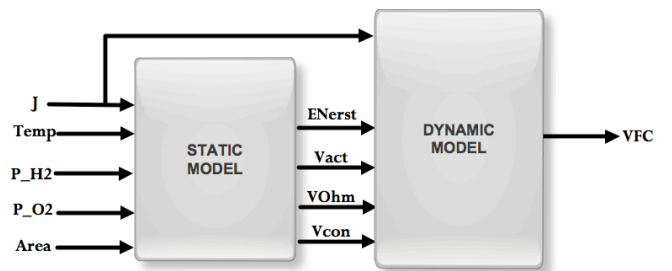


Fig. 2 – Model of the PEM fuel cell in Matlab/simulink

B. FUEL CELL CONVERTER

A. Selection of the topology

The electrochemical reactions involved in the fuel cell define its output power, which needs to be managed in order to be consistent with the requirements of each application [10-13]. In order to have an efficient conversion, a DC-DC converter is needed. According to [14], there are over 500 different topologies of DC-DC converters.

The selection of the topology is based on some significant criteria such as; 1) cost, 2) efficiency, 3) electrical isolation, 4) ripple free and 5) reliable operation. The efficiency depends of the conduction and switching losses. By reducing the number of components and their operating range this losses can be reduced. Switching losses can be also reduced using an adequate control, such as a soft switching technique either by zero-voltage switching (ZVS) or zero-current switching (ZCS) techniques.

Due to the low level of the fuel cell output voltage (19-24V) the boost ratio is very high and can't be achieved by a non-isolated boost converter; therefore, an isolated DC-DC converter topology with an isolated transformer is necessary. Then, the first requirement excludes all topologies without a transformer and also excludes all topologies for which a controller cannot be designed for a stable output voltage, during variations of output current and input voltage. The high transferred power involved is another requirement for choosing the configuration of the converter, because it results in a large size of the transformer and/or its saturation. For a compact, low cost and low weight converter, high-frequency operation is necessary because high-frequency operation reduces the size of transformer, filters and other reactive components [15].

With the high-frequency operation, the hard-switched converters suffer from high switching losses, electromagnetic interferences and component stresses. The switching losses increase with increase in switching frequency, reducing the efficiency of the converter. Therefore, soft switching is required for the operation of the converter at higher frequency in order to achieve higher efficiency.

Therefore, the topology selected for the application is represented in Figure 3 below, which corresponds to a full-bridge series-resonant inverter, followed by a high frequency transformer and a rectifier. Input and output filters are also considered to protect the fuel cell and the load of the ripples.

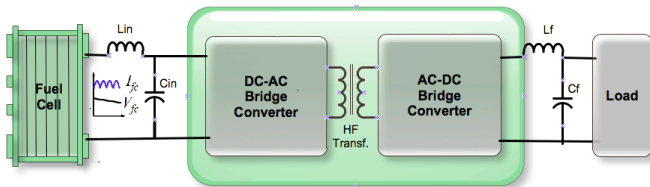


Fig. 3 – Topology of converter for the fuel cell application.

B. Operation of the series-resonant converter

The series resonant converter can operate in one of three possible modes, depending on the ratio of the operating frequency and resonance frequency namely;

- 1) Discontinuous-conduction mode (DCM) for $f_s < f_r/2$,
- 2) Continuous-conduction mode (CCM) for $f_r/2 < f_s < f_r$ and
- 3) Continuous-conduction mode (CCM) for $f_s > f_r$.

The operation can also be classified as below ($f_s < f_r$) or above ($f_s > f_r$) the resonance frequency f_r .

If the converter is operating below the resonance frequency, a phenomenon known as “zero current switching” occurs. The turn-off switching loss is zero but the turn-on switching loss is not zero. The transistors are turned on at high voltage. The capacitor impedance X_C dominates the impedance of the circuit Z with phase $\phi < 0$. The switch current is positive after the switching turn-on and is negative before switching turn-off.

If the converter is operating above resonance frequency a phenomenon known as “zero voltage switching” occurs. The driver forces the turn-off switch transition, while the turn-on transition is caused by the turn-off transition of the opposite transistor, not by the driver. Because turn-on transition occurs at zero voltage, the switching loss is zero, but there is a turn-off loss, however, this turn-off switching loss can be eliminated by a shunt capacitor to one of the transistors using a dead time in the drive voltages. The inductor impedance X_L dominates the impedance of the circuit Z and the current through the resonant circuit $i(t)$ lags the fundamental component of the voltage $V(t)$, with phase $\phi > 0$.

C. Control

The control structure of the converter is represented in Figure 4. This consists of two loops namely, the control of the voltage (which is a fast loop) and the control of the operation point of the PEM (which is a slow loop). The voltage controller is responsible of controlling the output voltage of the converter, keeping this in a constant value defined by the user even for load variations. The control of the PEM is responsible of controlling its operation, keeping it in its optimal point that is, producing the electrical power requested by the load with a minimum current and consequently with a minimum of hydrogen consumption.

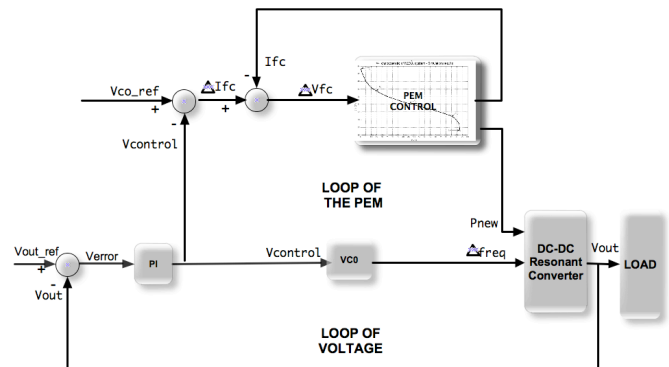


Fig. 4 – Scheme of the control structure of the resonant converter.

C. MATLAB/SIMULINK MODEL

The details of the model of the SRC in MatLab/Simulink software are presented while in the second part the simulation results are obtained and analyzed. Particularly, the results regarding to the dynamics of the system are presented to demonstrate that the system is fast in its dynamics and simultaneously guarantees the output voltage constant, even for load variations.

The model of the power generation system is performed in two parts, namely: the power circuit and the control circuit according to the circuit presented in Figure 1.1. The operation of the converter is already described in previous section.

A. Power circuit modeling

The elements of power converter are modeled in MatLab/Simulink according to the topology of converter selected and the tools provided by the software environment. The power elements are parameterized for its specific target, such as, DC sources, resistances, inductances, capacitors and power semiconductors such as diodes, Mosfets and IGBTs.

B. Control circuit modeling

The implementation of the control circuit in MatLab/Simulink is divided into two main subsystems: a subsystem to control the output voltage, which is composed by the modules of 1) Voltage control, 2) Frequency divider and 3) gate drive signals and a subsystem to control the operation point of the PEM composed by the PEM controller module. The detailed explanation of these modules is presented below.

C. Voltage Control circuit modeling

The voltage control subsystem allows at limiting the maximum and minimum values for the output voltage i.e., the control output signal, $V_{control}$, is always equal to zero (0), if $V_{out} > 750V$ (Selector #1), on the other side is always equal to one (1), if $V_{out} = 0V$ (Selector #2). Otherwise, the control module works according to the main goal for which it is designed, that is, through a PI controller and regardless the type and amount of load applied to the power system, it keeps the converter output voltage at 400V (Selector #3). This works as follows: the value of the output voltage (V_{out}) of the converter is measured and compared with the reference value; an error signal is produced and processed by the P - proportional I -integral controller producing the signal of

voltage control ($V_{control}$). The proportional term responds immediately to the error voltage yet typically cannot achieve the required set-point accuracy without an unacceptable large gain. On the other hand, the integral term yields an error zero in steady state for a constant set point and enables the rejection of disturbances.

D. Frequency divider and gate drive signals

This subsystem allows generating the four gate signals to the resonant inverter bridge, which changes accordingly to the signal reference. Once it is known the reference signal, interpreted as a voltage (V_{COref}), established by the PI controller, the module continues-time VCO generates a sinusoidal signal whose frequency shifts from the quiescent frequency parameter (f_c) with a sensitivity to the input parameter (k_c) and amplitude A_c . The inverter topology is a full-bridge; then four output signals need to be generated by this subsystem, one for each transistor respectively ($M_i, i = 1, 2, 3, 4$). They are synchronized by ϕ , which is the initial phase parameter and assumes zero or π value in the case.

E. Variation of the load

The scheme of figure 5 below was implemented to make fast load variations. Basically the auxiliary circuit changes the state of the IGBT2 and thus the value of the load presented to the converter. The diode D1 prevents circulation currents towards of the converter.

When switch control turns ON to OFF $\Leftrightarrow 1 \rightarrow 0 \Leftrightarrow R_{min}$ to $R_{max} \Leftrightarrow I_{max}$ to I_{min}

When switch control turns OFF to ON $\Leftrightarrow 0 \rightarrow 1 \Leftrightarrow R_{max}$ to $R_{min} \Leftrightarrow I_{min}$ to I_{max}

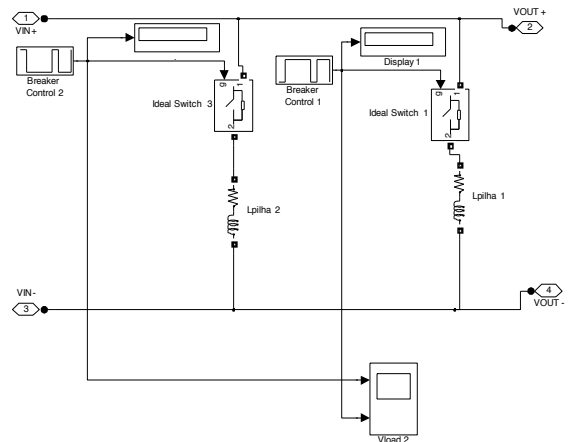


Figure 5 – Variation of the load subsystem.

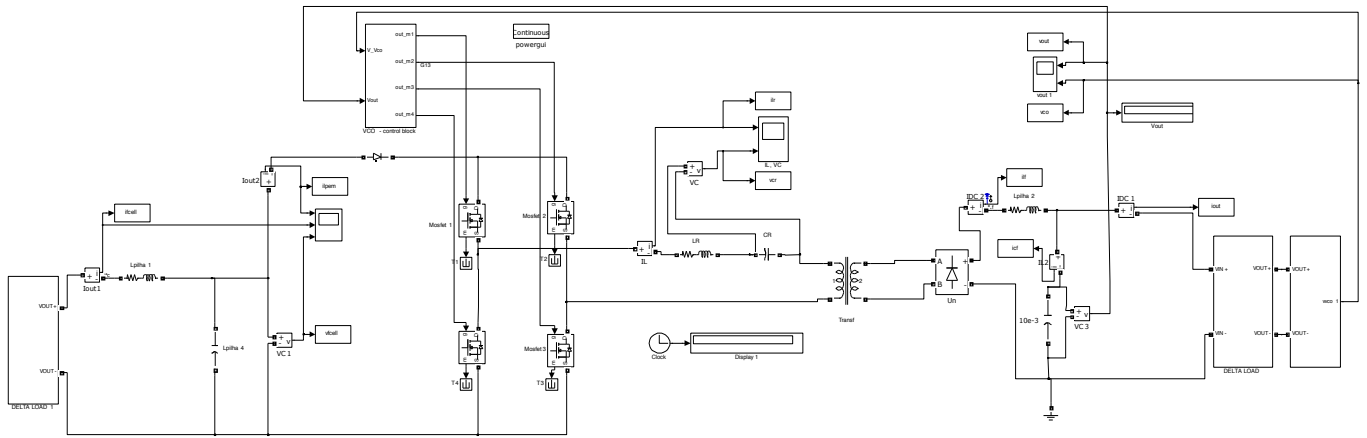


Fig. 6 – Scheme of SRC.

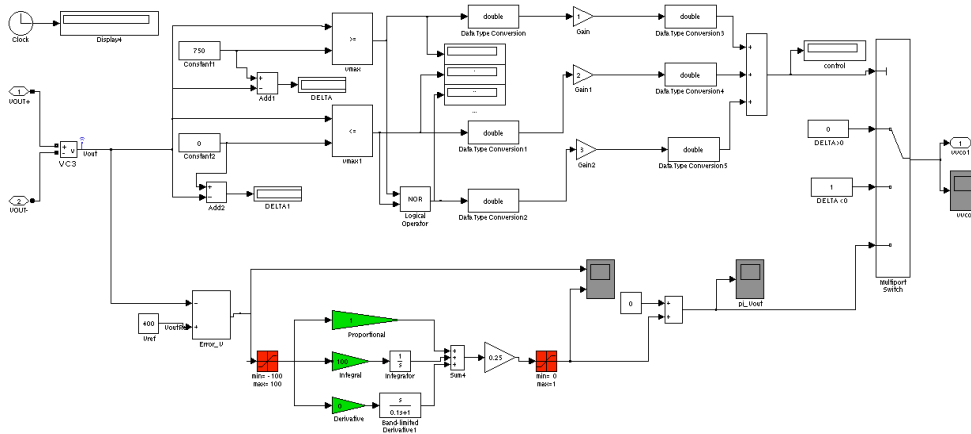


Fig. 7 – Scheme of the voltage control circuit.

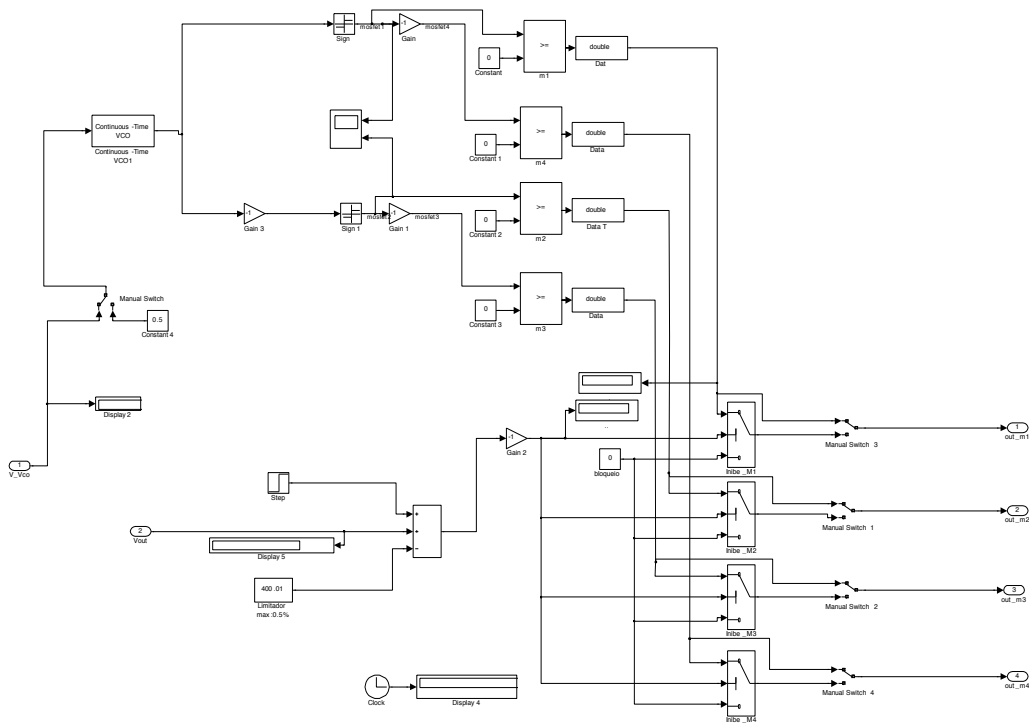


Fig. 8 – Scheme of the frequency divider and gate drive signals.

D. SIMULATION RESULTS

The main objectives to achieve in simulation are:

- 1) Validation of the stability of the output voltage controller, which should always guarantee a constant voltage even for loading variation in step-up, and step-down.
- 2) Validation of the system dynamics particularly, verifying if it is fast in its dynamics.

Accordingly, the variables such as; output voltage and current, control signal VCO, fuel cell voltage and current, and resonant circuit waveforms are analyzed.

A. Output voltage and current

The stability of the voltage controller is observed in Figure 6.12. It appears that for a variation of the load the output voltage of the converter remains constant. This condition is valid to both situations, to a step-up of load which occurs at 0.2 seconds at Figure 6.12 a) and to a step-down of load which occurs at 1.0 seconds at Figure 6.12 b).

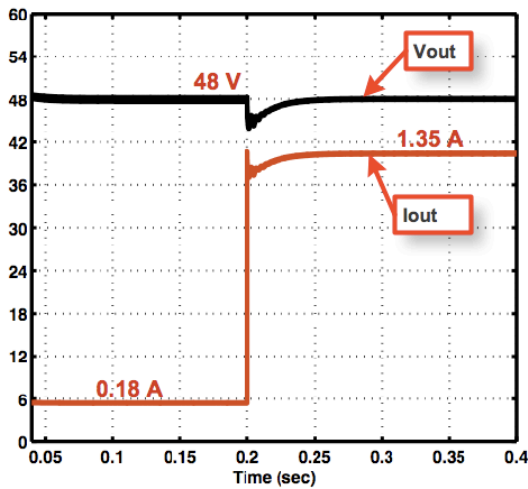


Fig. 9 – Output voltage and current – Simulation

B. Control signal – VCO

The dynamics of the system is evaluated by the response time of the system to load variations, which for the case is performed by the control signal –VCO established in the PI controller and sent as a reference to the frequency oscillator module in the simulation model, as explained above. Whence, observing the two situations of load variation present in Figure 6.13 a) and Figure 6.13 b), respectively it appears that the delay in time response of the VCO signal is approximately 10ms for the step-up while for the step-down the time response of the VCO signal does not present any delay. A small oscillation in the VCO signal appears just in step-up load condition, which proves that the parameters of the PI controller are well adapted to the system.

Knowing that the error is generated in Simulink by the expression, $\varepsilon = V_{\text{reference}} - V_{\text{measured}}$, the main goal of

the voltage controller is to minimize this error for any load variation, as is shown in the two figures below.

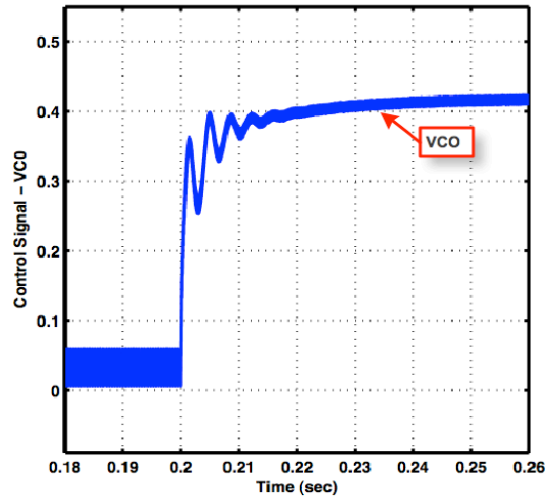


Fig. 10 – VCO signal- Simulation

C. Resonant circuit operation

Through the analysis of Figure 6.16 it appears that the operating frequency of the converter varies in accordance with the load requested to the system. The frequency increases in a step-up load condition (Figure 6.16 a)) and decreases in a step-down condition (Figure 6.16 b)). In dynamic terms it can be seen that the transition of the operating frequency is instantaneous, from whence it follows that the system has good dynamic in terms of frequency as expected from a resonant converter.

From Figure 6.16 it appears also that output voltage remains constant in both cases of load variation. This is extremely important since it satisfies one of the requirements imposed to the power system under study.

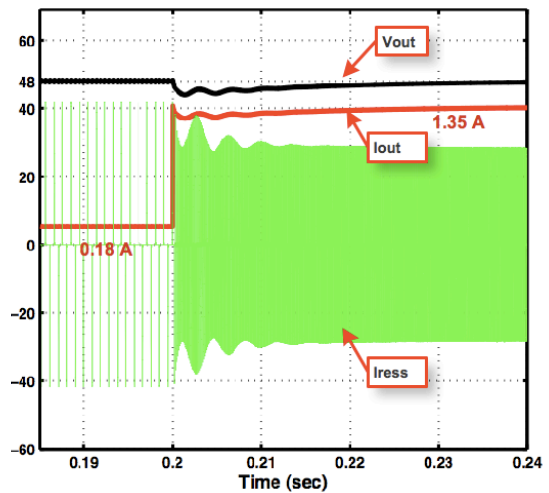


Fig. 11 – Resonant circuit variables.

D. Fuel cell voltage and current

In Figure 6.17 it is observed that the fuel cell current varies according to the variation imposed by the load that

is this rises for a step-up of current as observed in Figure 6.17 a) and drops to a step-down as observed in Figure 6.17 b). The fuel cell voltage drops when the current rises at the same instants in which the load variation occurs. The effect of the control is present in the both situations however its effect is more accentuated in the step-up condition. A small ripple appears in the fuel cell voltage function of the frequency operation of the converter. The ripple is smaller for the high load condition because of the increase of the frequency operation.

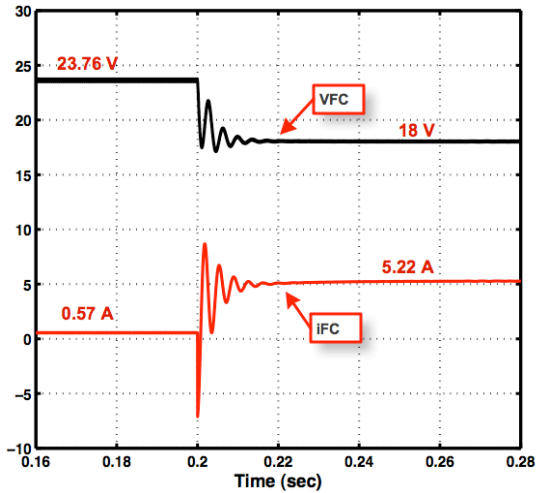


Fig. 12 – Fuel cell voltage and current.

E. EXPERIMENTAL RESULTS

In this section it is investigated the stability and the dynamics of the system. Accordingly, several variable waveforms are analyzed namely; the input voltage and current, the PI controller, the resonant current, which allows seeing a real change in the converter frequency corresponding to the load variation, and the output voltage.

The experimental setup used is represented in Figure 16 and corresponds to the topology of converter represented in Figure 19. The load is composed by a set of several resistors connected in series, whose variation is performed with a manual switch. The fuel pressure that provides a PEM stack is monitored by a standard dial pressure gauge, which maintains it constant in the range of 0.3 to 0.5bar. The ventilator is used to inject the oxidant flow necessary into the stack in order to produce the electrochemical reaction. The voltage of 26.06V represented by the multimeter corresponds to the open-circuit fuel cell voltage.

A. Analysis and discussion of the results

1. Input voltage and current

The input voltage in Figure 20 remains constant even for a step-up load variation, which proves the stability of the voltage loop. The effect of the controller is presented in

the input current, which as maximum oscillation amplitude of 8A, with a stabilization time of 3ms. The controller does not affect the input voltage.

2. Control signal PI

The dynamics of the system is evaluated by the analysis of the control signal PI. Then, considering the situation of load variation represented in Figure 21 it appears that the stabilization time of the PI controller is approximately 7ms. In addition it presents a small oscillation, which proves that the parameters of the PI control are well adapted to the system. The situation of Figure 18 is for a step-up load condition.

The error of voltage is given by $\varepsilon = V_{\text{measured}} - V_{\text{reference}}$, accordingly, the PI controller acts to minimize this error for any load variation, as is shown in the figure.

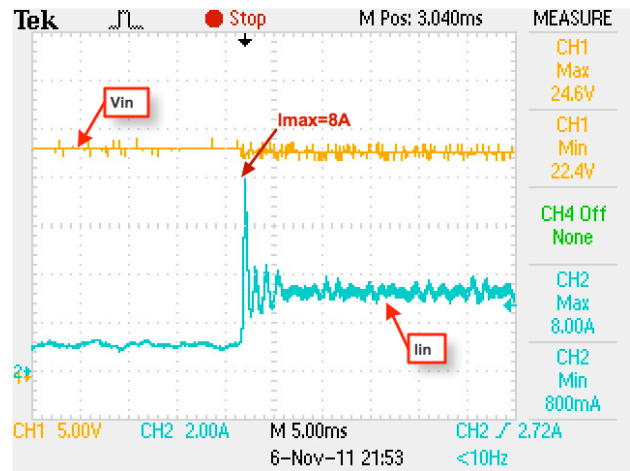


Fig. 13 – Input voltage and current – Experimental.

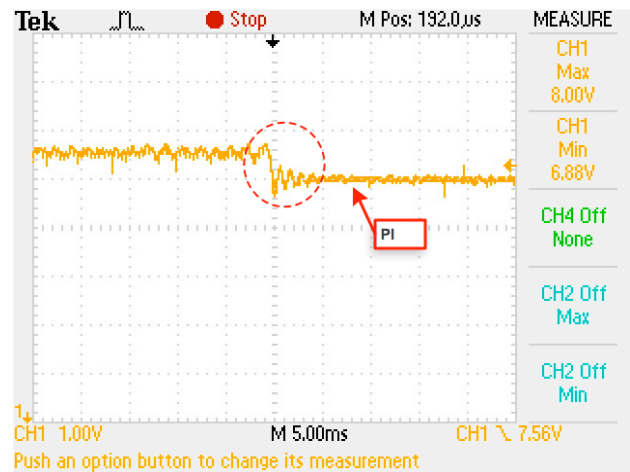


Fig. 14 – Dynamics of the PI controller– Experimental.

3. Resonant current

From the analysis of Figure 22, which corresponds a step-up load condition it follows that the converter reacts to the load variation, varying the operation frequency accordingly. Thus, for a small load level (I_{min} , R_{max}) the frequency is low while for a high load level (I_{max} , R_{min}) the

frequency is high. In dynamic terms it can be seen that the transition in the frequency of operation is instantaneous, hence, we conclude that the system has good dynamic characteristics. It can be also observed that even for the load variation the output voltage remains constant.

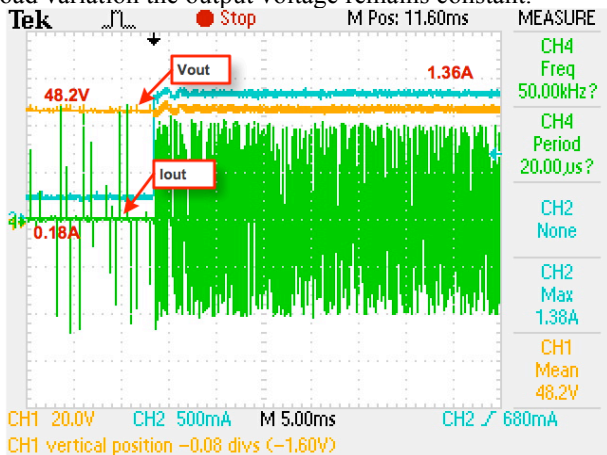


Fig. 15 – Resonant circuit variables– Experimental.

4. Output voltage and current

In the Figure 23 below it is validated the stability of the voltage control loop of the converter that is, it can be seen that it remains constant despite the variation of the load.

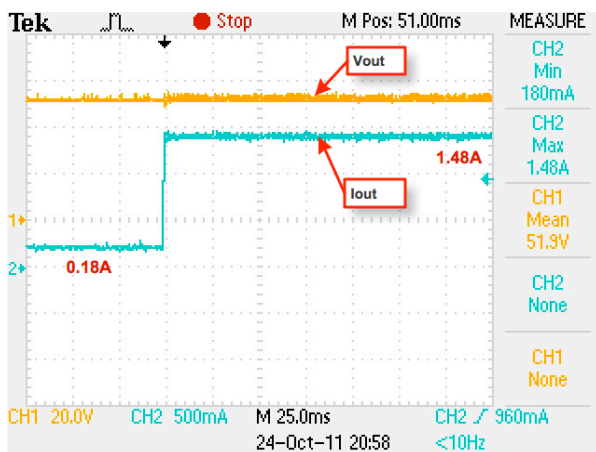


Fig. 16 – Output voltage and current – Experimental

F. CONCLUSIONS

Modeling and simulation techniques are indispensable in every aspect of power system design. Power systems need to be simulated in a longer period of time and more frequently especially when they are being analyzed using complex computer algorithms.

The implementation in MatLab/Simulink software is presented in a first part while in the second part the simulation results were discussed. A special attention is given to the control strategy, providing detailed explanation to each control subsystem, namely: the voltage control, the frequency control and PEM control. In a second part it is evaluated the performance of the power

generation system implemented in MatLab/Simulink. The analysis of the results is focused in the stability of the system, which was proved by the output voltage V_{out} , which remains constant even for the load variations imposed to the system. It was also proved that the resonant converter suits perfectly the changes imposed on the system by changing its operating frequency correspondently.

Finally, the analysis of the experimental results allows concluding that the system implemented provides excellent stability, robustness and good dynamic response making it a strong candidate for industrial applications in various areas of energy in accordance with the current tendencies in the sector.

REFERENCES

- [1] Trigg M. C., Nayar C. V., Matlab Simulink Modelling of a Single-Phase Voltage Controlled Voltage Source Inverter. *Electrical Engineering* (2006). p. 1-6. ISBN: 9781424416660.
- [2] Kashif Ishaque, Zainal Salam, Hamed Taheri. Accurate MATLAB Simulink PV System Simulator Based on a Two-Diode Model. *Journal of Power Electronics* 2010; 11(2): p.179-187.
- [3] <http://www.mathworks.com/>
- [4] Outeiro M.T., Chibante R., Carvalho A.S. and de Almeida A. T. A Parameter Optimized Model of a PEM Fuel Cell Including Temperature Effects. *Journal of Power Sources* 2008; 185(2):952-960.
- [5] Outeiro M. T., Chibante, R., Carvalho, A. S., de Almeida, A. T. , A new parameter extraction method for accurate modeling of PEM fuel cells *International Journal of Energy Research* 2008; 33(11):p 978-988.
- [6] Outeiro M. T., Chibante, R., Carvalho, A. S., "A novel soft-switching dc/dc converter applied to improve the efficiency of a PEM fuel cell system, 35th Annual Conference of the IEEE Industrial Electronics Society (IECON'09) 3-5 November, Porto, Portugal.
- [7] Abu-Qahouq J. Batarseh, I. . Generalized analysis of soft-switching DC-DC converters. *IEEE Proceedings of Circuits and Systems, ISCAS 2000, Geneva 2000.* 507-510.
- [8] Steigerwald, R.L., High frequency resonant transistor DC-DC converters. *IEEE Transactions on Industrial Electronics*, 1984. 31(2): p. 181-191.
- [9] Blaabjerg, F., Z. Chen, and S.B. Kjaer, Power Electronics as Efficient Interface in Dispersed Power Generation Systems. *IEEE Transactions on Power Electronics*, 2004. 19(5): p. 1184-1194.
- [10] Cancelliere, P., et al., Modeling and Control of a Zero-Current-Switching DC/AC Current-Source Inverter. *IEEE Transactions on Industrial Electronics* 2007. 54(4): p. 2106-2119.
- [11] Ivensky, G., et al., Reducing IGBT Losses in ZCS Series Resonant Converters. *IEEE Transactions on Industrial Electronics*, 1999. 46(1): p. 67-74.
- [12] Jin, K. and X. Ruan, Hybrid Full-Bridge Three-Level LLC Resonant Converter- A Novel DC-DC Converter Suitable for Fuel Cell Power System *IEEE Transactions on Industrial Electronics*, 2006. 53(5): p. 1492-1503.
- [13] Rong-Jong Wai and Rou-Yong Duan. . High-Efficiency Bidirectional Converter for Power Sources With Great Voltage Diversity. *IEEE Transactions on Power Electronics* 2007; 22(5):1986-1996.
- [14] Krykunov, O., *Comparison of the DC/DC-Converters for Fuel Cell Applications*. *International Journal of Electrical, Computer, and Systems Engineering*, 2007. 1(1): p. 71-79.
- [15] Rathore, A., A. Bhat, and R. Oruganti, *A Comparison of Soft-Switched DC-DC Converters for Fuel Cell to Utility Interface Application*. *IEEE Proceedings*, 2007: p. 588-594.